

Supplemental information

Figure S1

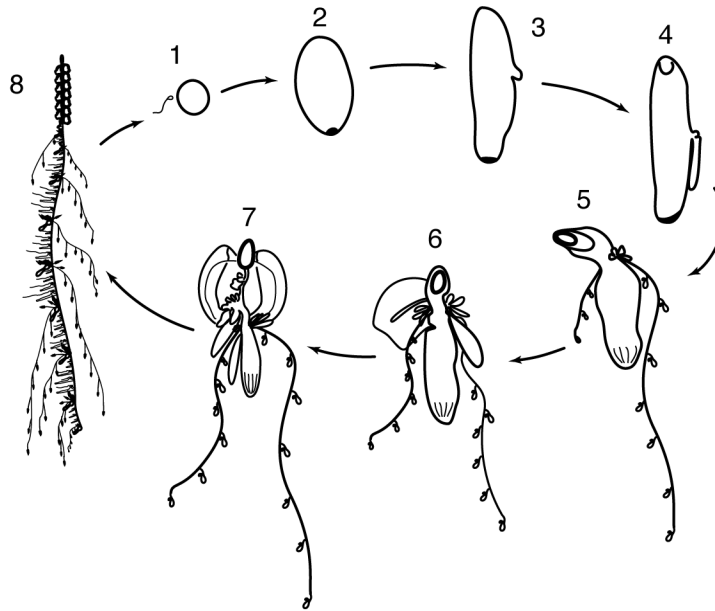


Figure S1. Lifecycle of *Nanomia bijuga*. 1. Egg and sperm. 2. 1.5 day old planula. 3. Two day old planula with larval tentacle bud. 4. 2.5 day old planula with forming pneumatophore and developing larval tentacle. The mouth opening of the protozoid is at the bottom. 5. One week old siphonula with pneumatophore and two larval tentacles bearing larval tentilla. 6. 20 day old siphonula with larval bract, and zooids developing on the ventral side of the protozoid indicating that growth zones have been established. 7. Young colony with first functional nectophore and zooids present along the elongating body of the protozoid. The elongating body of the protozoid corresponds to the future stem of the polygastric stage. 8. Mature colony – polygastric stage with multiple gastrozooids. Figure modified from [S1]. Original figure was adapted from [S2].

Figure S2A

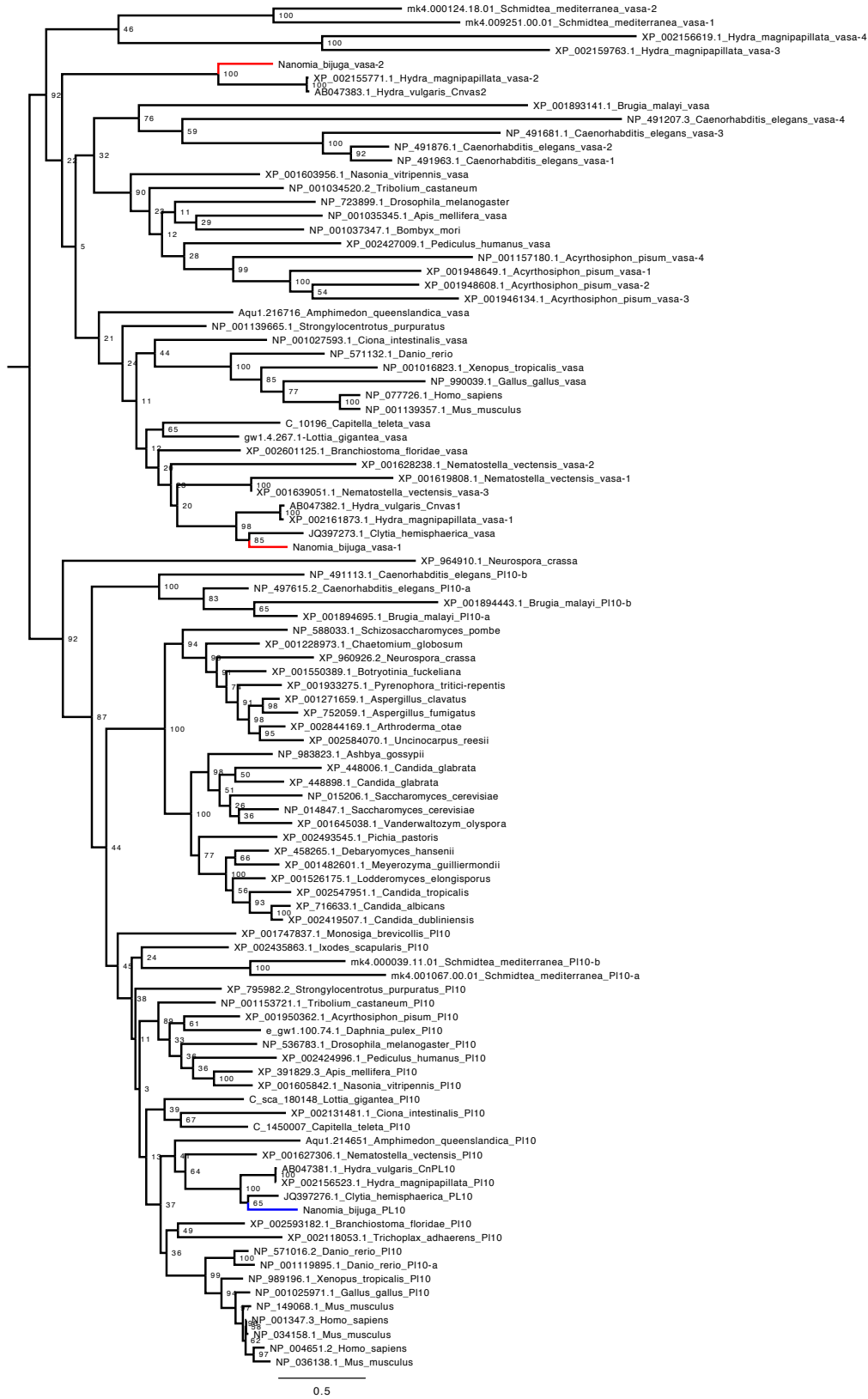


Figure S2B

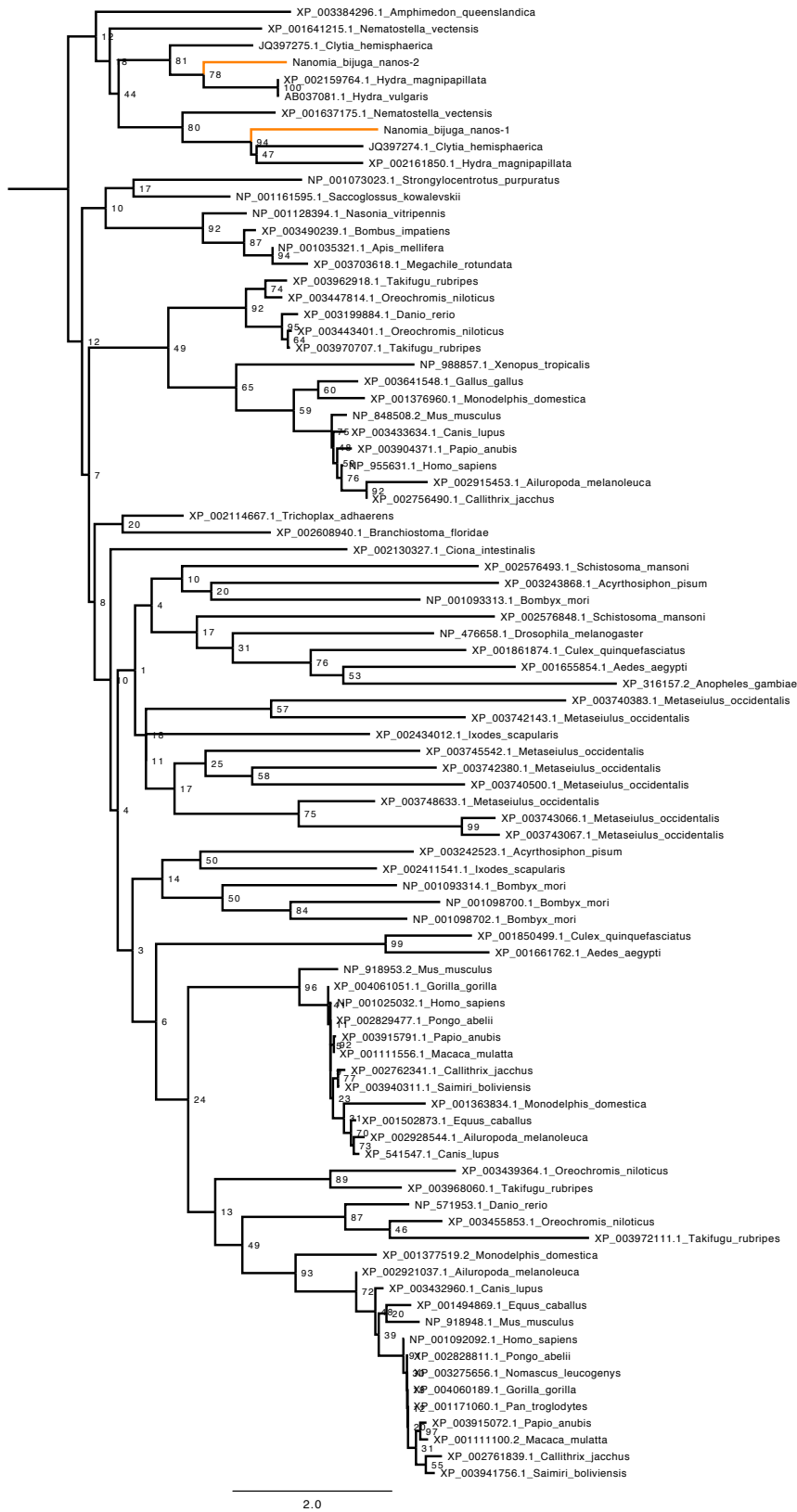


Figure S2C

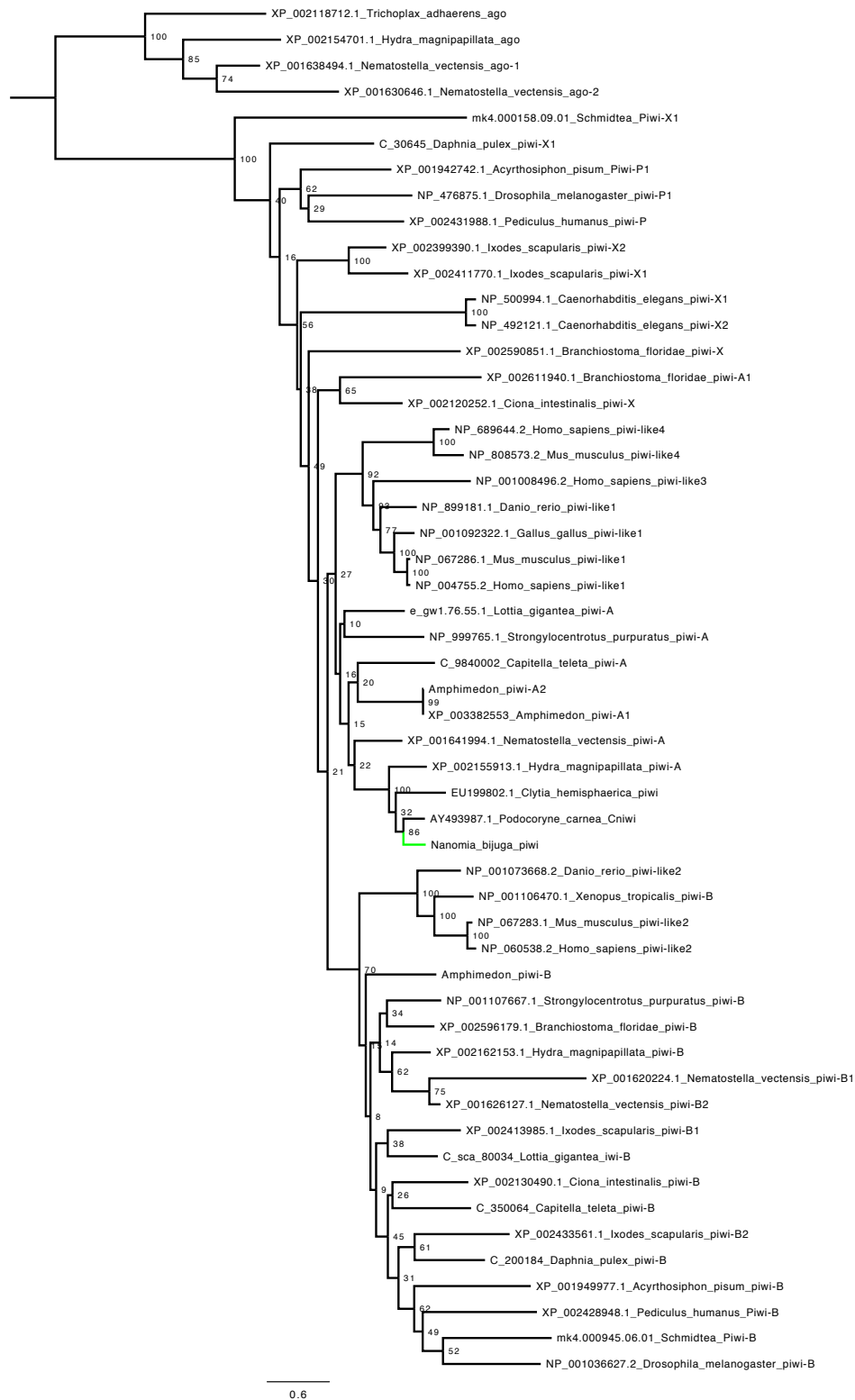


Figure S2. Phylogenetic analysis of select interstitial stem cell and germline genes in *Nanomia bijuga*. Maximum likelihood trees are shown: (A) *vasa-1*, *vasa-2* and *Pl10*, (B) *nanos-1*, *nanos-2* and (C) *piwi*.

Figure S3

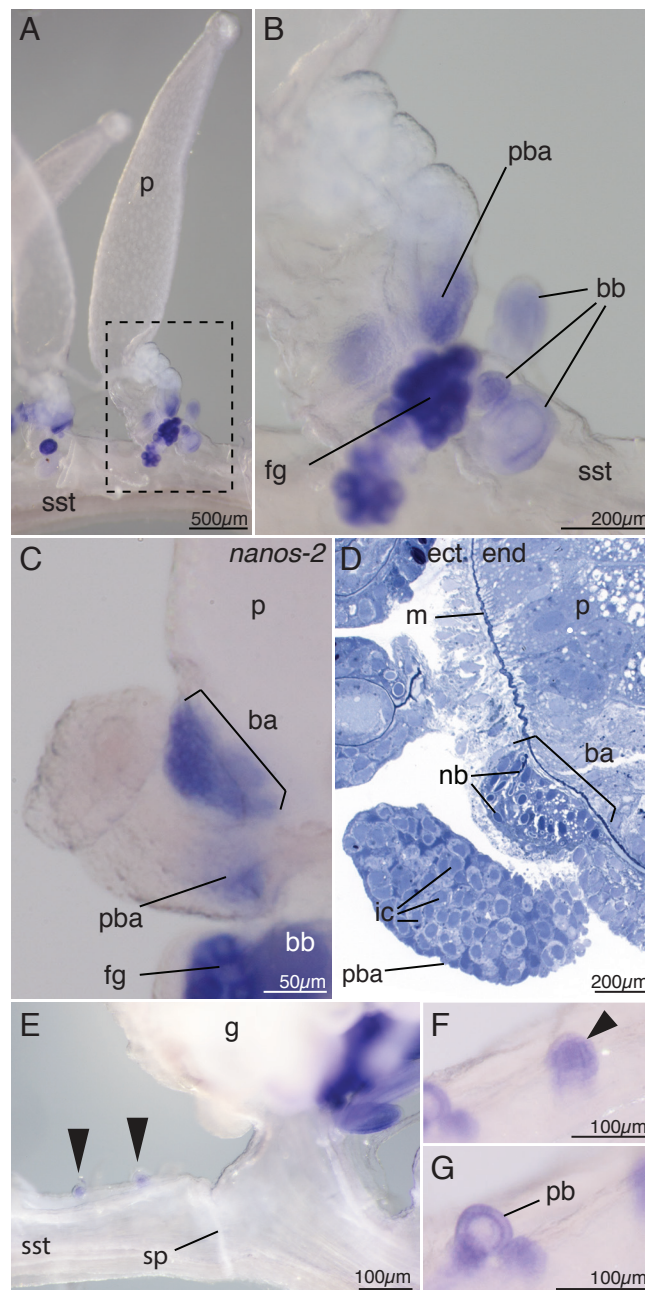


Figure S3. Palpons. (A-B) *vasa-1* transcript. (A) Mature palpon with *vasa-1* expression present exclusively in the papacle base. Anterior to the right. (B) Close up of the boxed region in A. *vasa-1* expression is restricted to the proximal end of the palpacle base and can also be found in accompanying developing bracts and female gonophores. (C) *nanos-2* transcript in the basigaster region and the palpacle base. Anterior to the left. (D) Semi-thin longitudinal section of the palpon base, stained with toluidin blue, reveals interstitial cells in the palpacle base and developing nematocysts in the basigaster region. Anterior to the left. (E) Clusters with *vasa-1* expression at the anterior end of a cormidium. The sphincter region marks the posterior end of a cormidium. At the site of the sphincter the hollow stem can be constricted. Anterior to the right. (F) Close-up of an early palpon cluster bud (arrowhead). (G) Close-up of a later developmental stage of a palpon cluster with the palpon bud visible in the center and further buds laterally. ba: basigaster; bb: bract bud; ect: ectoderm; end: endoderm; fg: female gonodendron; ic: interstitial cell; m: mesoglea; p: palpon; pb: palpon bud; pba: palpacle base; sp: sphincter; sst: siphosomal stem.

Figure S4. Expression pattern of *vasa-1*. Sense controls are labeled within the figure. Anterior regions or distal regions in case of zooids are up. (A,B) Nectosomal growth zone. (C,D) Siphosomal growth zone and anterior part of the siphosome. (E) Mature gastrozoid with expression in the tentacle base and forming tentilla. (F) Close-up of tentacle base shown in E. (G) Close-up of palpacle base. (H) Mature palpon. (I) Mature gastrozoid. (J) Mature female gonodendron. (K) Male gonodendron with four gonophores in different developmental stages. (L) Young female gonodendron. (M) Young male gonophore. b: bract; ba: basigaster; fg: female gonodendron; g: gastrozoid; h: horn of the growth zone; mgo: male gonophore; ne: nectophore; nst: nectosomal stem; p: palpon; pba: palpacle base; pn: pneumatophore; sst: siphosomal stem; tba: tentacle base.

Figure S5. Expression pattern of *nanos-2*. Sense controls are labeled within the figure. Anterior regions or distal regions in case of zooids are up. (A,B) Nectosomal growth zone. (C,D) Siphosomal growth zone. (E,F) Anterior part of the siphosome. (G) Mature cormidium with mature female and male gonophores. (H) Gastrozoid. (I) Close-up of tentacle base shown in H. (J) Proximal end of a palpon with palpacle base. (K) Tentacle base. (L) Palpacle base. (M) Cell cluster with *nanos-2* expression at the site of gonodendron formation at the base of a palpon. (N) Developing bean-shaped female gonodendron. (O) Developing female gonodendron starting to spiral. (P) Mature female gonodendron. (Q) Male gonodendron with three gonophores. (R) Mature female gonodendron. (S) Male gonophores. ba: basigaster; fg: female gonodendron; g: gastrozoid; goc: gonodendron cell cluster; h: horn of the growth zone; mgo: male gonophore; ne: nectophore; nst: nectosomal stem; p: palpon; pba: palpacle base; pn: pneumatophore; sst: siphosomal stem; tba: tentacle base.

Figure S6. Expression pattern of *PL10*. Sense controls are labeled within the figure. Anterior regions or distal regions in case of zooids are up. (A,B) Nectosomal growth zone. (C) Siphosomal growth zone. (D) Siphosomal growth zone and anterior part of the siphosome. (E) Siphosomal growth zone with horn. (F) Anterior part of the siphosome. (G,H) Mature gastrozoid. (I,J) Mature palpon. (K,L) Mature female gonodendron. (M,N) Male gonodendron. ba: basigaster; fg: female gonodendron; g: gastrozoid; h: horn of the growth zone; mgo: male gonophore; ne: nectophore; nst: nectosomal stem; p: palpon; pba: palpacle base; pn: pneumatophore; sst: siphosomal stem; tba: tentacle base.

Figure S4

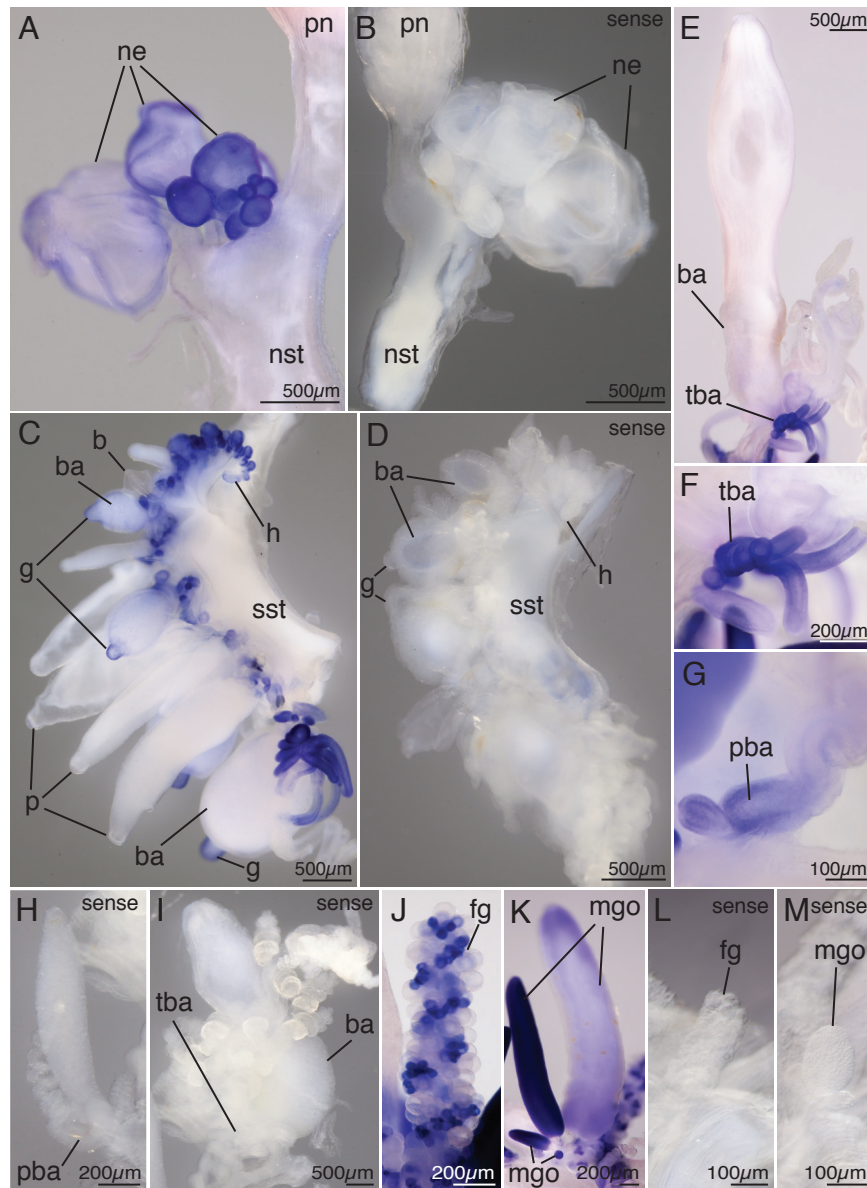


Figure S5

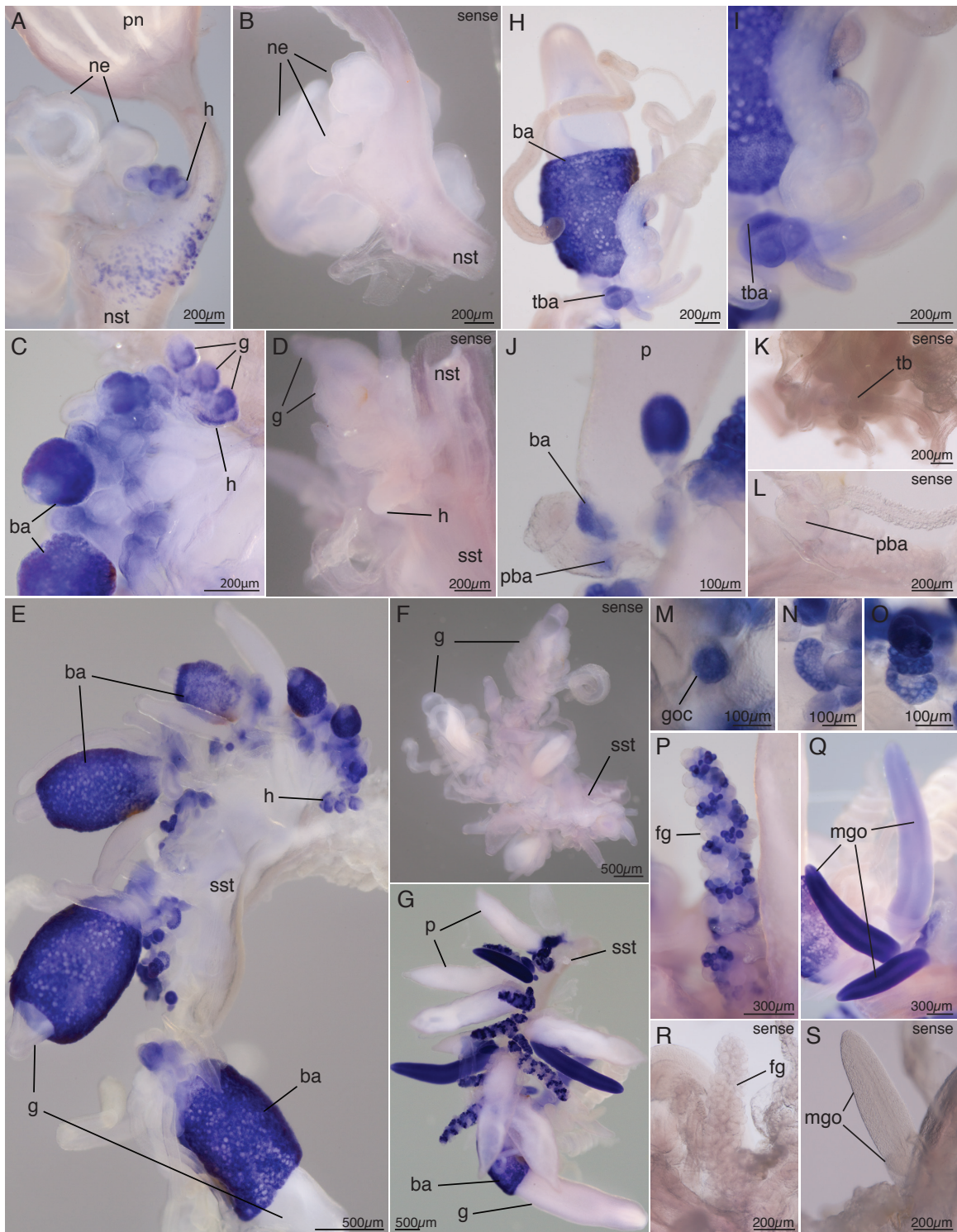


Figure S6

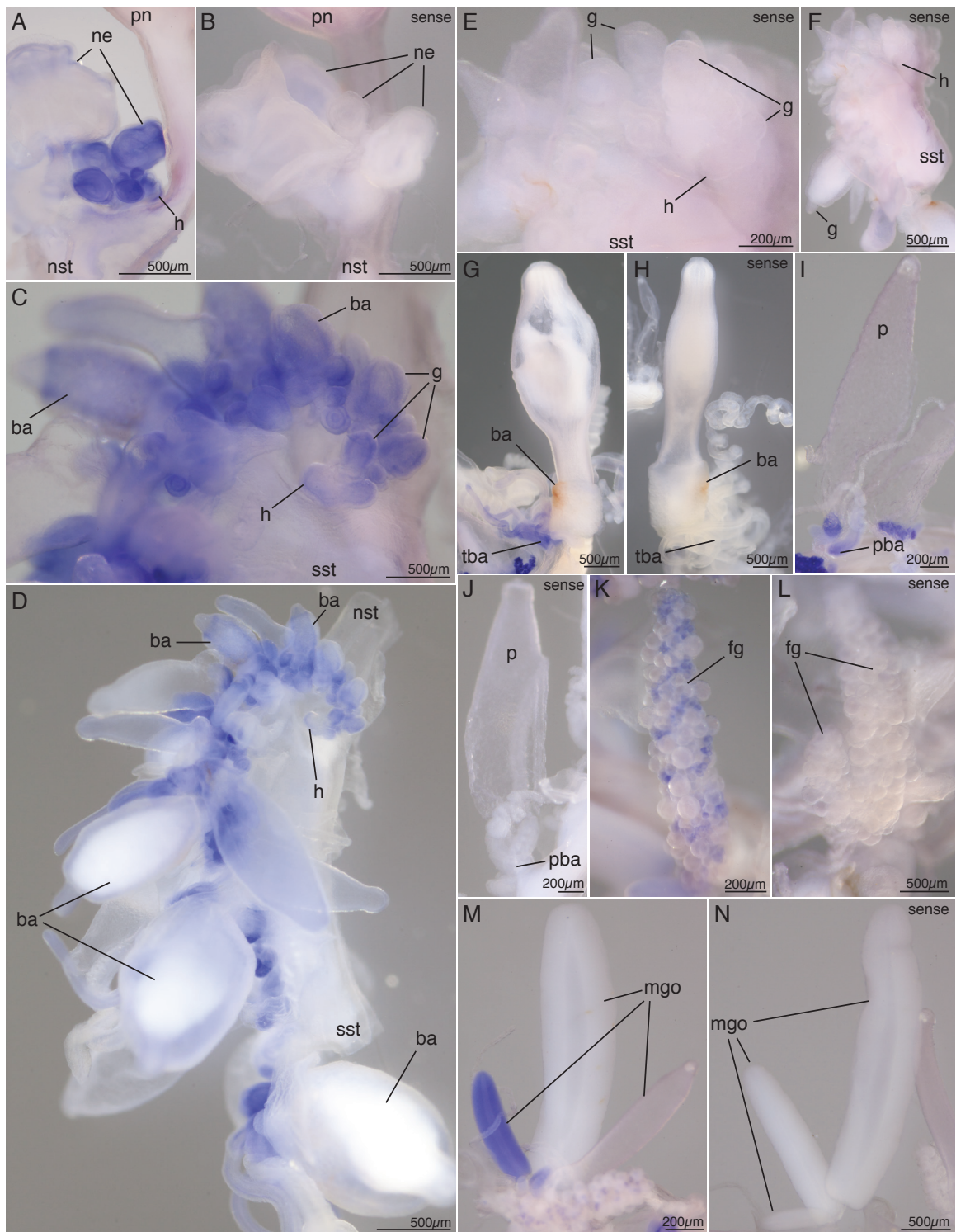


Figure S7

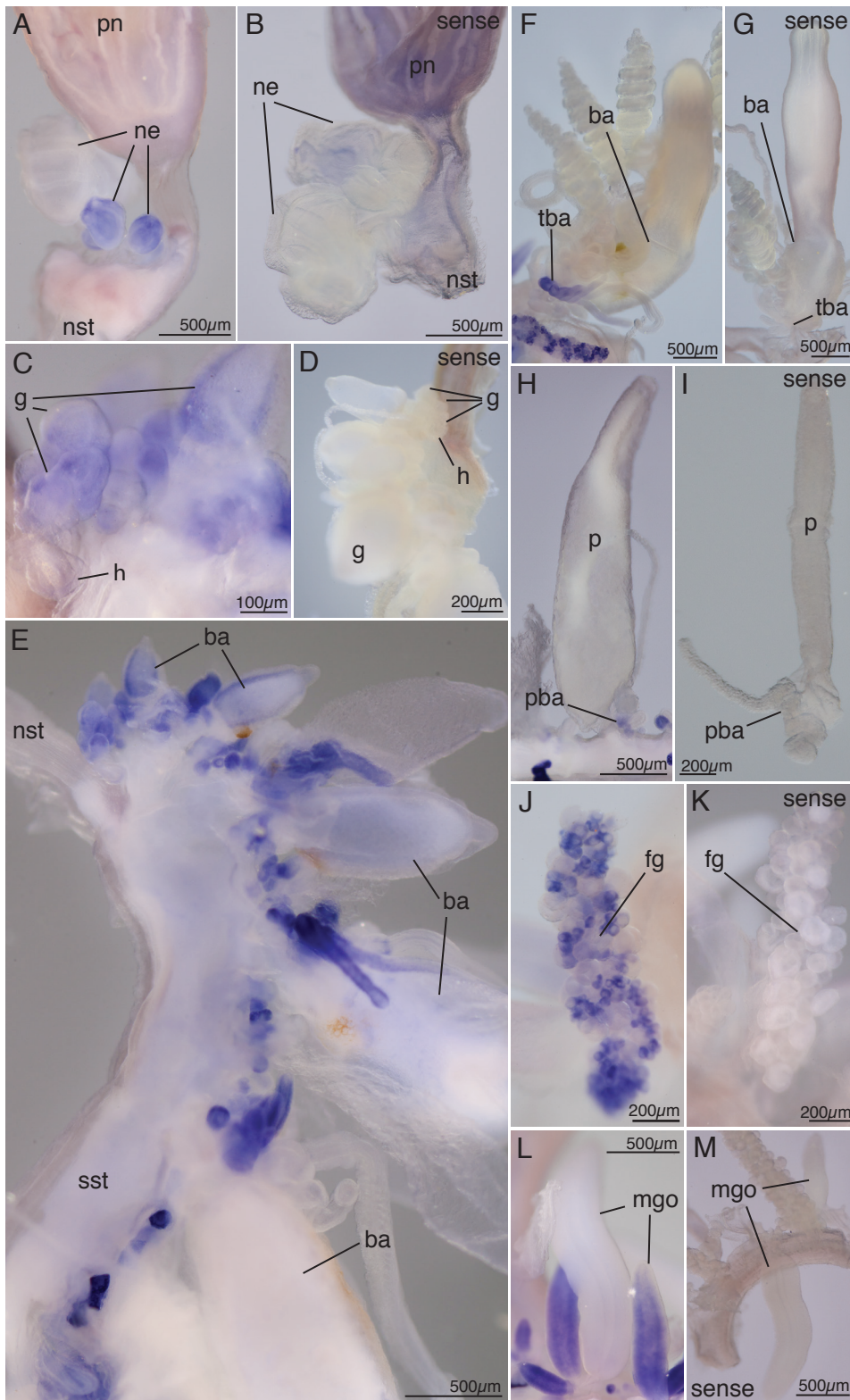
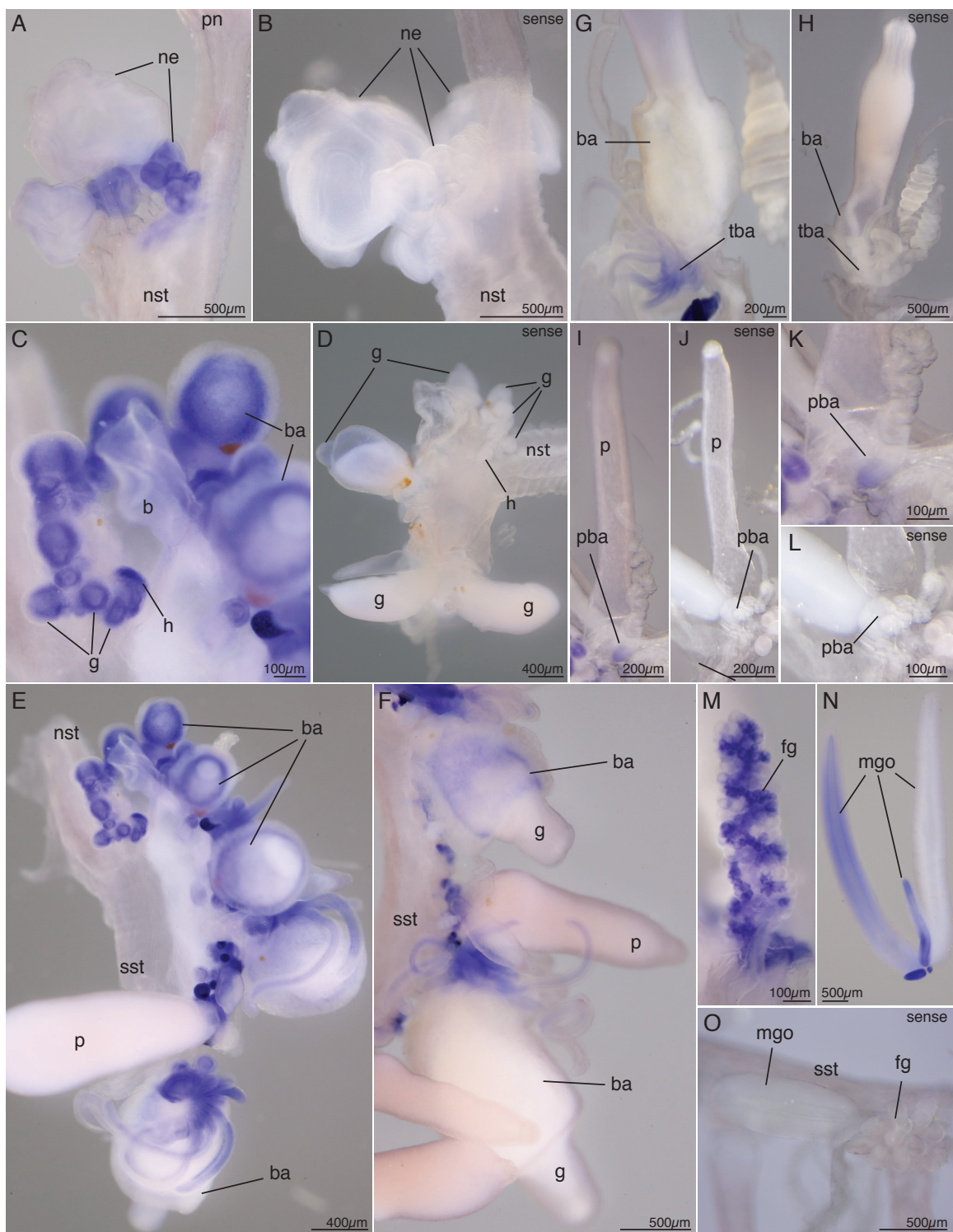


Figure S7. Expression pattern of *nanos-1*. Sense controls are labeled within the figure. Anterior regions or distal regions in case of zooids are up unless stated otherwise. (A,B) Nectosomal growth zone. Some unspecific signal could be observed within the pneumatophore of the sense control. (C) Siphosomal growth zone. (D) Siphosomal growth zone and anterior part of the siphosome. (E) Siphosomal growth zone and anterior part of the siphosome. (F,G) Mature gastrozoid. (H,I) Mature palpon. (J,K) Mature female gonodendron. (L) Male gonodendron. (M) Male gonophores. Lateral view of the stem. ba: basigaster; fg: female gonodendron; g: gastrozoid; h: horn of the growth zone; mgo: male gonophore; ne: nectophore; nst: nectosomal stem; p: palpon; pba: palpacle base; pn: pneumatophore; sst: siphosomal stem; tba: tentacle base.

Figure S8. Expression pattern of *piwi*. Sense controls are labeled within the figure. Anterior regions or distal regions in case of zooids are up unless stated otherwise. (A,B) Nectosomal growth zone. (C) Siphosomal growth zone. (D) Siphosomal growth zone and anterior part of the siphosome. (E) Siphosomal growth zone and anterior part of the siphosome. (F) Subsequent siphosomal fragment. *piwi* expression could be found in the basigaster region of the gastrozoid at the top but not in the gastrozoid more posteriorly. (G,H) Mature gastrozoid. (I,J) Mature palpon. (K) Close-up of palpacle base shown in I. (L) Close-up of palpacle base shown in J. (M) Mature female gonodendron. (N) Mature male gonodendron. (O) Male gonophore and young female gonodendron. Lateral view of the stem. Dorsal is up. b: bract; ba: basigaster; fg: female gonodendron; g: gastrozoid; h: horn of the growth zone; mgo: male gonophore; ne: nectophore; nst: nectosomal stem; p: palpon; pba: palpacle base; pn: pneumatophore; sst: siphosomal stem; tba: tentacle base.

Figure S8



Supplemental Experimental Procedures

Collection of Nanomia bijuga specimens

Nanomia bijuga specimens were collected from the floating dock in front of Friday Harbor Labs (FHL), San Juan Island, WA (12-19 June 2011) and in Monterey Bay, California, and adjacent waters. In Monterey Bay specimens were collected on 29 Sep 2012 via blue-water diving from a depth of 10–20 m and on December 28 Sep 2012 to 03 Oct 2009 by ROV Doc Ricketts (R/V Western Flyer) at depths ranging from 348 - 465m. After collection specimens were kept in filtered seawater (FSW) overnight at 8°C in the dark.

Identification and Amplification of interstitial stem cell/germ cell marker genes

We used tblastx to identify *Nanomia bijuga* homologous for *piwi*, *nanos-1*, *nano-2*, *vasa-1* and *PL10* in a *Nanomia bijuga* transcriptome reference using available sequence information from *Clytia hemisphaerica*, *Podocoryne carnea* and *Hydra vulgaris*. Sequences for the *Nanomia bijuga* orthologs have been submitted to Genbank (Accession Nos. KF790888-790893).

Sequence alignments and phylogenetic analysis

To identify homologous genes to *piwi*, *nanos-1*, *nano-2*, *vasa-1* and *PL10* across Animalia, we relied on estimates of statistically significant sequence similarity [S3] using the BLAST package [S4]. Initially, we queried the nucleotide sequence of each of these genes in *Nanomia bijuga* against the SwissProt and NCBI RefSeq databases using blastx and default parameters for sequence comparison (scoring matrix, gap opening/extension). Once we inferred the correct open reading frame in our sequences, we queried the translated amino acid sequences using blastp with the BLOSUM80, BLOSUM62 and BLOSUM50 scoring matrices. For each gene, a subset of significant blast hits that matched the sampling in Kerner et al. [S5] was used for phylogenetic analyses. We used MUSCLE v3.8.31 [S6] to generate multiple sequence alignments for each gene separately, except for PL10 and vasa that were combined into a single matrix because they are sister gene families [S5]. RAxML v7.5.7 [S7] was used for phylogenetic analysis with the WAG model of amino acid substitution and the Γ model of rate heterogeneity. We used the non-parametric bootstrap [S8] with 500 replicates for each matrix to assess support on each gene tree. The source code for the phylogenetic analyses, as well as the input fasta sequence files for all considered sequences and the output trees in newick format, are available as a git repository at https://bitbucket.org/caseywdunn/siebert_etal. Complete program settings can be found within these files.

Whole mount RNA in situ hybridization

In situ hybridization was performed on both Friday Harbor and ROV collected specimens and yielded the same expression patterns. ROV specimens are presented in the figures since gonodendra were in more mature stages. Specimens were transferred into a Petri dish coated with Sylgard 184 (Dow Corning Corporation) and relaxed by adding isotonic 7.5 % $\text{MgCl}_2 \cdot 6\text{H}_2\text{O}$ in Milli-Q water at a ratio of approximately $\frac{1}{3}$ MgCl_2 and $\frac{2}{3}$ FSW. After pinning them out in a stretched position using insect pins (Austerlitz Insect Pins, 0.2mm, Fine science tools) they were fixed in 0.5% glutaraldehyde/4% paraformaldehyde (PFA) in FSW for two minutes and incubated in 4% PFA in FSW overnight at 4°C. Mature nectophores and bracts tend to get detached when handling specimens in the dish and were therefore not accessible for analysis in all cases. Specimens were then washed for three times in Ptw (phosphate buffer saline and 0.1% Tween). Dehydration was performed using EtOH with 15 min washes in 25% EtOH/PTw, 50% EtOH/PTw, 75% EtOH/Milli-Q water, 2x 100% EtOH and then transferred to MetOH and stored at -20°C. Use of EtOH for dehydration was empirically found to minimized tissue sloughing, detachment of endoderm from ectoderm.

Dig-labeled probes were generated using Megascript T7/SP6 kits (Life Technologies). Probe lengths were as follows: *nanos-1*: 800; *nanos-2*: 954; *PL10*: 1,233, *piwi*: 1,389; *vasa-1*: 1,381. Primer used for probe generation were:

	forward	reverse
<i>nanos-1</i>	GAACACTCGCTAGTTGCTGTG	TCTATCGGTTTTAACTTTTGGTG
<i>nanos-2</i>	AGTAGTGGGAGCAGCCAATG	AACCGTTGGTGGATTGATTC
<i>PL10</i>	ACTGCTGCATTTTGGTTCC	TGCCTGTTGCTGGTTGTATG
<i>piwi</i>	CATGCTGTGTGCTGATGTTG	GCAAAGGCCTCTTTGAATTG
<i>vasa-1</i>	TTCCGGACTATTGCTCAAGG	GATCCCAGCCATCATCATTC

Working concentration of mRNA probes were 1ng/ml. *In situ* hybridizations were performed according to the protocol described by Genikhovich and Technau [S9] with few deviations. Starting at step #27, the specimens were incubated in MAB instead of PTw. The blocking buffer composition was MAB with 1% BSA and 25% sheep serum. Anti-Digoxigenin-AP, Fab fragments (Cat.No.11093274910, Roche Diagnostics) were used in 1:2000 dilution in blocking buffer. After antibody binding the specimens were washed in MAB instead of PBT. Once the NBT/BCIP development was stopped with water, the samples were stored overnight in 100% ethanol followed by storage in PBS. Samples were stable in PBS for many weeks provided that the medium was exchanged regularly to prevent bacterial growth. Photodocumentation was performed using Canon MP-E 65mm Macro lens or using stereomicroscope Leica S8APO. In case of Figure 2A,4C a stacking strategy was applied to increase depth of field. Four photographs with different focal planes were merged using function “auto blend layers” in Adobe Photoshop CS 5.5. After all photo documentation was completed, specimens were

stored in 4% PFA/PBS and the integrity of the signal has remained stable. This is a preferable long-term storage because the tissue structure is preserved. Whole mounts were difficult to mount because of size of tissue fragments. When trying to permanently mount tissue in Euparal (BioQuip Products, Inc) the mounting procedure caused tissue damage and strong afterstaining occurred despite several washes in water after stopping the staining reaction. Absence of signal within the stem or mature bodies could be due to probe penetration problems. When analyzing *in situ* signals, special attention was paid to sites where the stem had been cut and mature zooids were purposely sliced prior to the start of the *in situ* protocol. No *in situ* signal could be detected at these cutting sites.

Thick and ultrathin sectioning for transmission electron microscopy

Specimens fixed as described above were washed with PBS five times for 15 min each and afterwards stored at 4°C in the presence of sodium azide ([1ng/ml]). Specimens were postfixed in 2% glutaraldehyde, 4% paraformaldehyde, 100mM sucrose and 100 mM sodium cacodylate buffer (SCB). After three washes in 100 mM sucrose, 100mM SCB for 15 min each were postfixed in 1% OsO₄, 100mM sucrose, 100mM SCB. Tissue was processed for resin embedding according to the manufacturer's instructions (Low viscosity embedding Kit, Cat. 14300, Electron Microscopy Sciences). All washes and incubations were conducted at slow agitation on a rocker table. Thick sections (0.5-0.750µm) were prepared using glass knives, dried and counterstained in toluidin blue (0.1%) in sodium borate (1%) buffer. Ultra thin sections were prepared using a diamond knife. TEM images were acquired on Phillips 410 Transmission Electron microscope.

Supplemental References

- S1. Goetz, F. E. (2013). Nanomia life cycle. Available at:
http://commons.wikimedia.org/wiki/File:Nanomia_life_cycle_vector_wikimedia.svg.
- S2. Carré, D. (1969). Etude histologique du developpement de Nanomia bijuga (Chiaje, 1841), siphonophore physonecte, Agalmidae. Cah. Biol. Mar., 325–341.
- S3. Pearson, W. R., and Wood, T. C. (2007). Statistical significance in biological sequence comparison. In Handbook of Statistical Genetics, D. J. Balding, M. Bishop, and C. Cannings, eds. pp. 40–66.
- S4. Altschul, S. F., Gish, W., Miller, W., Myers, E. W., and Lipman, D. J. (1990). Basic local alignment search tool. J. Mol. Biol. 215, 403–410.
- S5. Kerner, P., Degnan, S. M., Marchand, L., Degnan, B. M., and Vervoort, M. (2011). Evolution of RNA-Binding Proteins in Animals: Insights from Genome-Wide Analysis in the Sponge Amphimedon queenslandica. Mol. Biol. Evol. 28, 2289–2303.
- S6. Edgar, R. C. (2004). MUSCLE: multiple sequence alignment with high accuracy and high throughput. Nucleic. Acids. Res. 32, 1792–1797.

- S7. Stamatakis, A. (2006). RAxML-VI-HPC: maximum likelihood-based phylogenetic analyses with thousands of taxa and mixed models. *Bioinformatics* 22, 2688–2690.
- S8. Felsenstein, J. (1978). Cases in which parsimony or compatibility methods will be positively misleading. *Syst. Zool.* 27, 401–440.
- S9. Genikhovich, G., and Technau, U. (2009). In Situ Hybridization of Starlet Sea Anemone (*Nematostella vectensis*) Embryos, Larvae, and Polyps. *Cold Spring Harbor Protocols* 2009, pdb.prot5282–pdb.prot5282.